C40

Piezoelectric Energy Harvester Using Wake Induced Vibration

Javad Farrokhi Derakhshandeh, PhD **Yousef Gharbia, PhD** **Nima Gharib, PhD**

ABSTRACT

This paper investigates the wake-induced vibration of a thin piezoelectric (PZT) actuator in a laminar flow regime to explore the utilization of vortex energy in energy harvesting. In this study, the selected Reynolds number is 200 and the study focuses on the impact of vortices at different longitudinal spacing ratios. The longitudinal spacing ratio, represented as GR =L = L/D, ranges from 3.0 to 6.0, where D is the diameter of the cylinder and L is the longitudinal distance between the cylinder and the tip of the PZT. The flexible PZT in the wake of the cylinder behaves as a cantilever beam, while the upstream cylinder remains stationary. The frequency of vortex shedding is found to vary depending on the characteristics of boundary layers and vortices in the wake for different GR values. The results demonstrate that based on the GR the imposed forces on the PZT varies which can affect the deformation of the PZT and consequently harvested power output.*

INTRODUCTION

The main objective of this paper is to explore the phenomenon of wake-induced vibration (WIV) in a flexible plate known as PZT actuator that is positioned in the wake region of the bluff body to capture the vortices energy. PZT materials have high sensitivity and can generate electricity through mechanical strain, as well as experience mechanical strain when subjected to an electrical charge. A thin film of a PZT can be used as 'eels", for instance, to harness the mechanical motion of traveling vortices behind a bluff body. As a result, the conversion of ambient and aeroelastic vibrations into a usable form of electric power has been suggested as a means of powering various electronic components, including microelectromechanical systems, actuators, and wireless sensors used for health monitoring purposes and military (Mehmood 2013, Koyvanich et al. 2015, and Zhang et al. 2021). Consequently, the proposed methodology offers advantageous opportunity to generate the requisite power by capitalizing on the freely available energy that is produced by Von Karman Street (VKS) in the wake region. This methodology can present a novel approach to harvesting energy that is not only efficient and cost-effective but also can minimize the reliance on non-renewable sources of energy. While numerous investigations have been conducted in the scientific literature pertaining to the Flow-Induced Vibration (FIV), in general (Bernitsas et al. 2008 and Derakhshandeh et al. 2016), the operation of a flexible plate or PZT to harness the energy of vortices has received less attention. This concept is still in its early stages of development, and our understanding of it has primarily evolved over the past two decades (Ramm and Wall 1998, Akaydin et al. 2010, Dai et al. 2014, Hu et al 2018, Shan et al. 2019, and Zhao et al. 2021, Meng et al. 2021). Ramm and Wall (1998) conducted a comprehensive investigation on the fluid-structure interaction (FSI) model, specifically focusing on the vortex-induced vibration (VIV) of a flexible thin plate connected to a square cylinder. The study revealed that the plate displayed a recurring response characterized by periodic oscillations. Notably, the peak amplitudes at the plate's tip reached

Dr. Javad Farrokhi Ph.D. is associate professor in the Department of Mechanical Engineering, American University of the Middle East, Kuwait. Dr. Yousef Gharbia Ph.D. is associate professor in the Department of Mechanical Engineering, American University of the Middle East, Kuwait. Dr. Nima Gharib Ph.D. is assistant professor in the Department of Mechanical Engineering, American University of the Middle East, Kuwait.

approximately 1D. Here, D was equal to the edge length of the square.

The phenomenon of the WIV has been also the subject of numerical investigations conducted by Sahu al. (2019). They specifically explored WIV in a cylinder with an attached plate under a 2D incompressible flow condition. The range of reduced velocities investigated by the authors varied from 1 to 70. It was observed that the presence of an attached plate on the circular cylinder led to the identification of three distinct flow regimes: vortex-induced vibration, steady flow, and galloping.

FIV phenomena comprising VIV and WIV were also investigated by Zhang and Wang (2016) using an energy harvesting device comprising a circular cylinder and two thin piezoelectris. The VIV experiment revealed a positive correlation between voltage output and load resistance. The authors observed that the vibration frequency of the smaller cylinder was influenced by the shedding frequency of vortices from the larger upstream cylinder. Furthermore, they identified a specific gap between the cylinders that optimized voltage and power output. In contrast, the lock-in region of WIV, affected by the larger diameter of the upstream cylinder, shifted backward, necessitating slightly higher wind speeds to achieve maximum power output. Particularly, they observed that WIV exhibited a higher produced power and proved more effective in enhancing the PZT power output of the examined energy harvesting device, surpassing the performance of VIV (Zhang and Wang, 2016).

This paper aims to conduct a thorough analysis of wake-induced vibrations (WIV) in a flexible plate and explore the complex fluid-structure interaction (FSI) involving a Piezoelectric Transducer. This investigation is carried out using a two-way fluid-structural interaction (TW-FSI) methodology, which ensures accurate modeling and simulation of the coupled behavior between the fluid flow and the PZT structure on a real time. Through the study, the impact of the PZT's location in the cylinder wake is examined, and the obtained results are subsequently compared and analyzed. Furthermore, the study goes beyond the fundamental analysis by examining the influence of the PZT's position within the wake of the cylinder. This examination involves the consideration of two distinct test cases to evaluate and compare the resulting effects. By varying the location of the PZT within the cylinder wake, the author seeks to gain insights into the relationship between its position and the observed deformation behavior. These comparative analyses can provide valuable information for further understanding the FSI characteristics and optimizing the performance of PZTs in wake-induced vibration scenarios.

NUMERICAL REPRODUCTION

The 3D model of the flow domain over the coupled fixed cylinder and a flexible plate (which acts as a piezoelectric (PZT)) is shown in Figure 1. The height and width of the domains are large enough and were set at 20 D and 50 D, respectively. Parameter D of 10 mm is the diameter of the cylinder. These large domains can provide accurate convergence without blocking effects (Alam et al. 2018 and Derakhshandeh et al. 2014). The conditions of both upside and downside walls of the domain were set in Fluent with no shear stress. The inlet velocity was adjusted to achive Re = 200, while the outlet boundary was specified to have no pressure and velocity gradients.

The fixed end of the PZT (AB in Figure 1) implies that the flexible plate can be treated as a cantilever beam subjected to a distributed force. As the flow passes over the cylinder, the generated vortices impose a non concentrated force on both sides of the PZT. Consequently, the wake of the cylinder generates Von Karman Street (VKS), causing the PZT to deform either upwards or downwards. The magnitude of the PZT deformation determines the corresponding change in the generated voltage.

The thin PZT with the dimensions of 0.4 (mm) thickness and 4D = 40 (mm) length is located in the wake region downstream of the cylinder. All charactristics of the model are presented in Table 1.

MATHEMATICAL MODEL

To solve the model, the Navier-Stokes (NS) equations for incompressible laminar flow are employed, which can be given by:

$$\nabla . u^{*} = 0, \tag{1}$$

$$\frac{\partial u^{*}}{\partial t^{*}} + (u^{*} . \nabla) u^{*} = -\nabla P^{*} + \frac{1}{Re} (\nabla^{2} u^{*}) \tag{2}$$

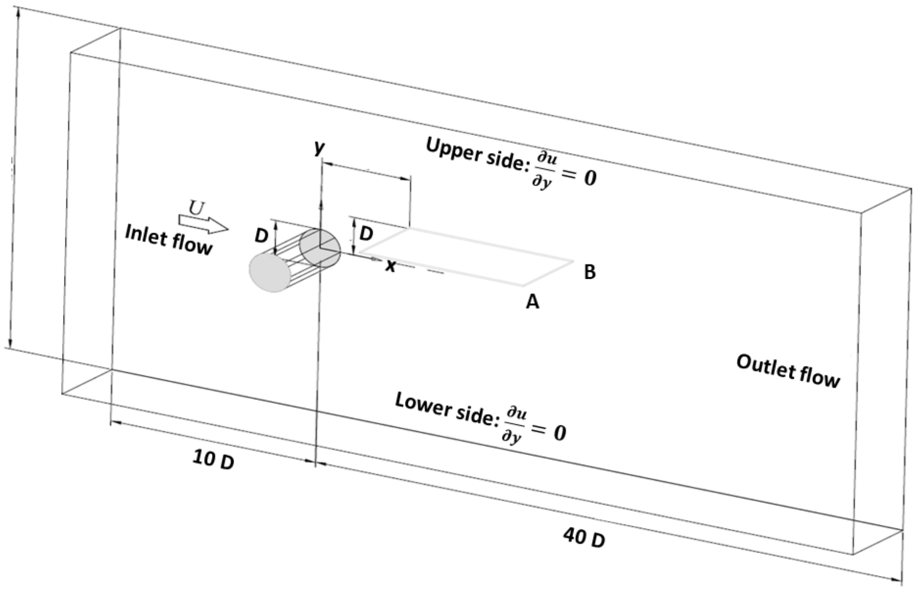

Figure 1 Numerical domain showing the boundary conditions and dimensions.

Table 1. The charactristics of the model applied in ANSYS Workbench for numerical analysis.

Physical item	Parameters	Characters/Values (units)
Flexible plate or PZT	Thickness	$t = 4\times10^{-3}$ (m)
	Span	$S = 4\times10^{-2}$ (m)
	Width	$W = 0.005$ (m)
	Mass	$m = 0.00012$ (kg)
	Stiffness	$k = 1100$ (N/m)
	Natural frequency	$f = 5.89$ (Hz)
	Young's Modulus	E = 2000000 (Pa)
	Shear Modulus	G = 746200 (Pa)
	Bulk Modulus	BM = 2083300 (Pa)
	Poisson's Ratio	$\nu = 0.34$

As previously stated, the deflection of the plate can be modeled using a narrow cantilever beam. This allows the vertical movement of the flexible plate or PZT to be simulated as a 1DOF of mass-spring-damper system. The subsequent equations offer a means to assess the deformation of the PZT, providing valuable insight into its behavior.

$$M(x) = EI\frac{d^2y}{dx^2} \tag{3}$$

$$EI\frac{dy}{dx} = \int_0^x M(x)dx + C_1 \tag{4}$$

$$EIy = \int_0^x dx \int_0^x M(x)dx + C_1x + C_2. \tag{5}$$

$$M(x) = -\frac{1}{2}\, F_x.(x)^2 \tag{6}$$

Hence:

$$EI\frac{d^2y}{dx^2} = -\frac{1}{2}\, F_x.(x)^2 \tag{7}$$

In the above equestions, the moment is denoted by M, and the polar moment and Young modulus of inertia are denoted by I and E, respectively. Hence, the equation describing the moment can be formulated as a function of the distributed load, as presented in Equation (6). By integrating Equation 7, and considering the boundary condition of the plate, the slope of the PZT actuator can be obtained. Considering the boundary condition of the PZT in this study, specifically when x = L and the slope is dy/dx = 0, and y = 0 at x = L resulting in the coefficients of $C_1 = \frac{1}{6}\,\omega L^3$, and $C_2 = -\frac{3}{24}\,F_x\,L^4$. Therefore, the deformation of the PZT can be written as:

$$y(t,x) = -\frac{F_x}{24EI}\,(x^4 - 4L^3x - 3\,L^4) \tag{8}$$

FSI SIMULATION

The primary focus of this research is on a complex fluid-structure interaction (FSI) problem. The fluid chosen for the experiment was water, characterized by a density of 998.2 kg/m³ and a dynamic viscosity of 0.001003 kg/(m·s). To verify the model, due to lack of available data with such a complex coupled system in literature, initially the authors examined the model for the flow over a single cylinder at Re = 200. Therefore, the extensive availability of data greatly enhances the verification process for the selected coupled system in this paper.

Mesh structure and quality analysis. To ensure the accuracy of the numerical data, grid sensitivity examinations were conducted to evaluate the flow passes a circular cylinder. The numerical data, summarized in Table 2, confirmed the appropriateness of the chosen mesh elements. These mesh elements were selected based on their similarity to those utilized in a previous study by Derakhshandeh (2022) on a single circular cylinder at Re = 200. Comparing the results, generally, it was observed that the maximum deviation error between the fluidic parameters obtained using different mesh types (1), (2), and (3) was negligible. Consequently, mesh type (2) was chosen for the rest of numerical investigations.

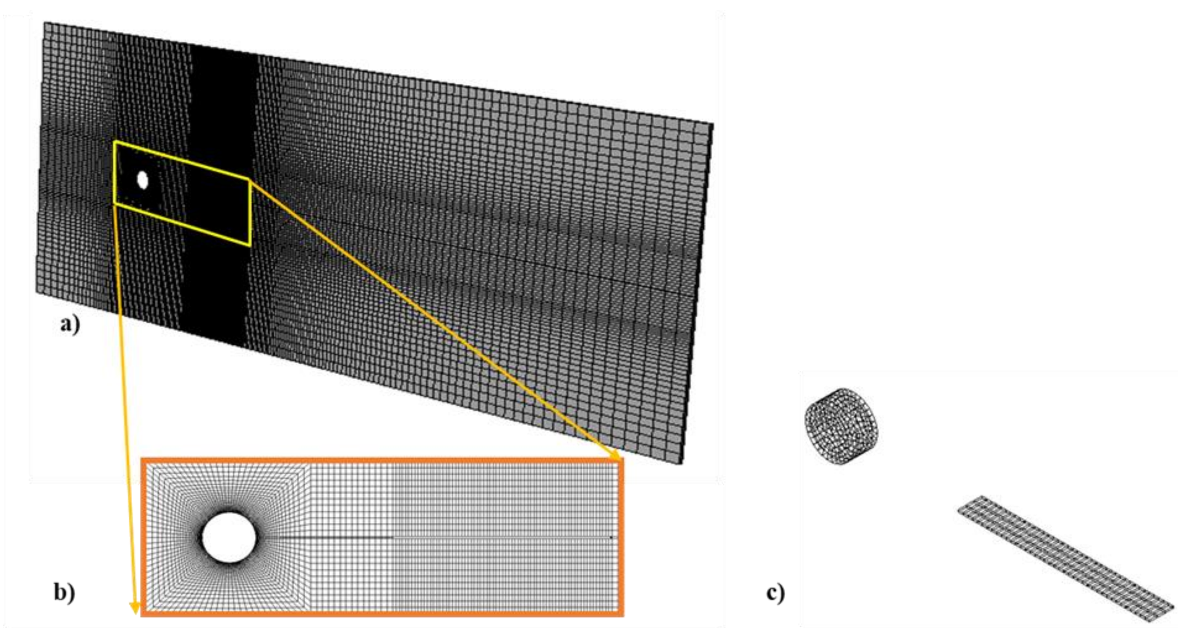

Figure 2 Mesh grid around the coupled cylinder and flexible plate; a) entire domain, b) zoom in area around the cylinder and plate in fluid region; c) solid parts.

Results verification. To ensure the accuracy of the model, extensive simulations were conducted for the flow over a single cylinder. The obtained numerical results were then carefully compared with published data, as presented in Tables 3. This rigorous comparison encompassed various fluidic parameters, including force coefficients and Strouhal numbers. Notably, the findings revealed a good agreement between the present study and the previously published data. This agreement serves as a strong indication of the model's reliability and its ability to accurately capture the flow characteristics and associated parameters.

Table 2. Mesh sensitivity results of flow over a circular cylinder at Re = 200.

Mesh Structure	Mesh type(1) ≈44,000 mesh elements	Mesh type(2) ≈ 65,000 mesh elements	Mesh type(3) ≈ 92,000 mesh elements
C_L	0.460	0.562	0.564
C_D	1.135	1.299	1.303
St	0.175	0.197	0.199

Table 3. Verification of the results for a circular cylinder when Re = 200.

Studies	C_D	C_L	St
Meneghini et al. (2001)	1.30	0.605	0.196
Dehkordi et al. (2011)	1.16	0.575	0.179
Derakhshandeh and Gharib (2021)	1.31	0.565	0.198
Present study	1.34	0.501	0.202

REULTS AND DSISCUSSIONS

Pressure field around the coupled cylinder and PZT. Figure 3 illustrates the variation of the instantaneous pressure coefficient at different time. The countour plots demonstrate that the pressure wake in the flow undergoes changes over time. Notably, the flexible PZT experiences differential pressure on its top and bottom surfaces. In Figure 3a, the development of the pressure behind the cylinder and its impact on the flexible PZT is depicted. At this stage, there is a relatively balanced pressure distribution, resulting in no significant deflection of the PZT. However, as the pressure difference between both sides of the PZT increases, the PZT starts to deform. The figure identifies three key locations: P_1 (corresponding to a very low pressure), P_2 (representing high pressure), and P_3 (associated with low pressure). These points are indicated in Figure 3c and 3d as the centers of pressure with dash-line circles. The displacement of these pressure points (e.g., P_1, P_2, and P_3) on both sides of the plate surfaces leads to varying pressure and consequently forces applied to the flexible PZT, ultimately causing its deflection. Consequently, the deflection of the PZT is directly proportional to the shedding frequency of vortices.

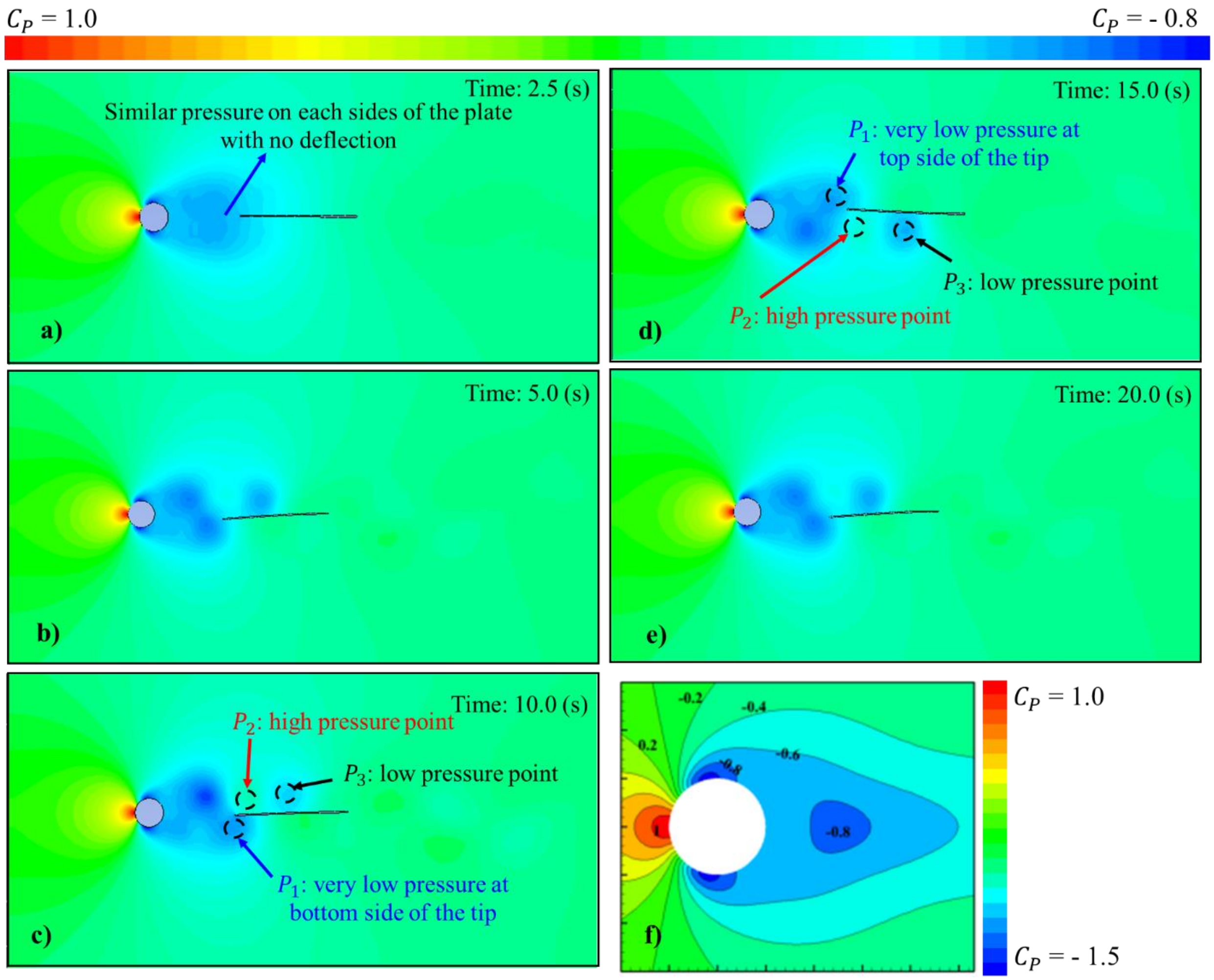

Figure 3 The distribution of the instantaneous pressure coefficient (C_P) at Re = 200; a-e): around the coupled circular cylinder and flexible PZT at various time steps, f) around single cylinder.

Figure 4 displays the time series of the C_L for both the cylinder (represented by the red plots) and the plate (represented by the blue plots) as a function of L*. This provides a more comprehensive understanding of the imposed forces and wake pressure. It is found that the cylinder and PZT exhibit minimal C_L at L* = 3.0 D and 3.5 D, respectively. As L* increases to 4.5 D, the oscillation of the lift coefficients for both the cylinder and PZT becomes more stable. Additionally, the amplitude of C_L substantially increases. However, beyond L* = 4.0 D, the gap ratio has a minimal effect on the C_L of the ctylinder and plate.

Deformation of the PZT due to imposed lift force. As shown in the previous section (Figure 4), due to the imposed lift force on the flexible PZT, this actuater can be deformed in y- direction. Figure 5 shows a sinosiudal deformation of PZT including a time history (Figure 5a) and 3D contour plots of downward and upward deformations (e.g., Figures 5b and 5c) for L* = 4.0. It is worth noting that the temporal evolution of the deformation exhibits a resemblance to the pressure and lift variations depicted in the previous figures (see Figure 3 and 4). Once the deformation of the PZT tip has been analyzed, the next step is to calculate the voltage generated by the PZT. This computation entails taking into account the specific parameters of capacitance and electromechanical coupling coefficient to accurately assess the voltage magnitude. By incorporating these factors, the resulting power output values might be determined. Hence, the wake-induced vibration (WIV) phenomenon can be regarded as a viable renewable energy source capable of generating electricity using the flexible PZT.

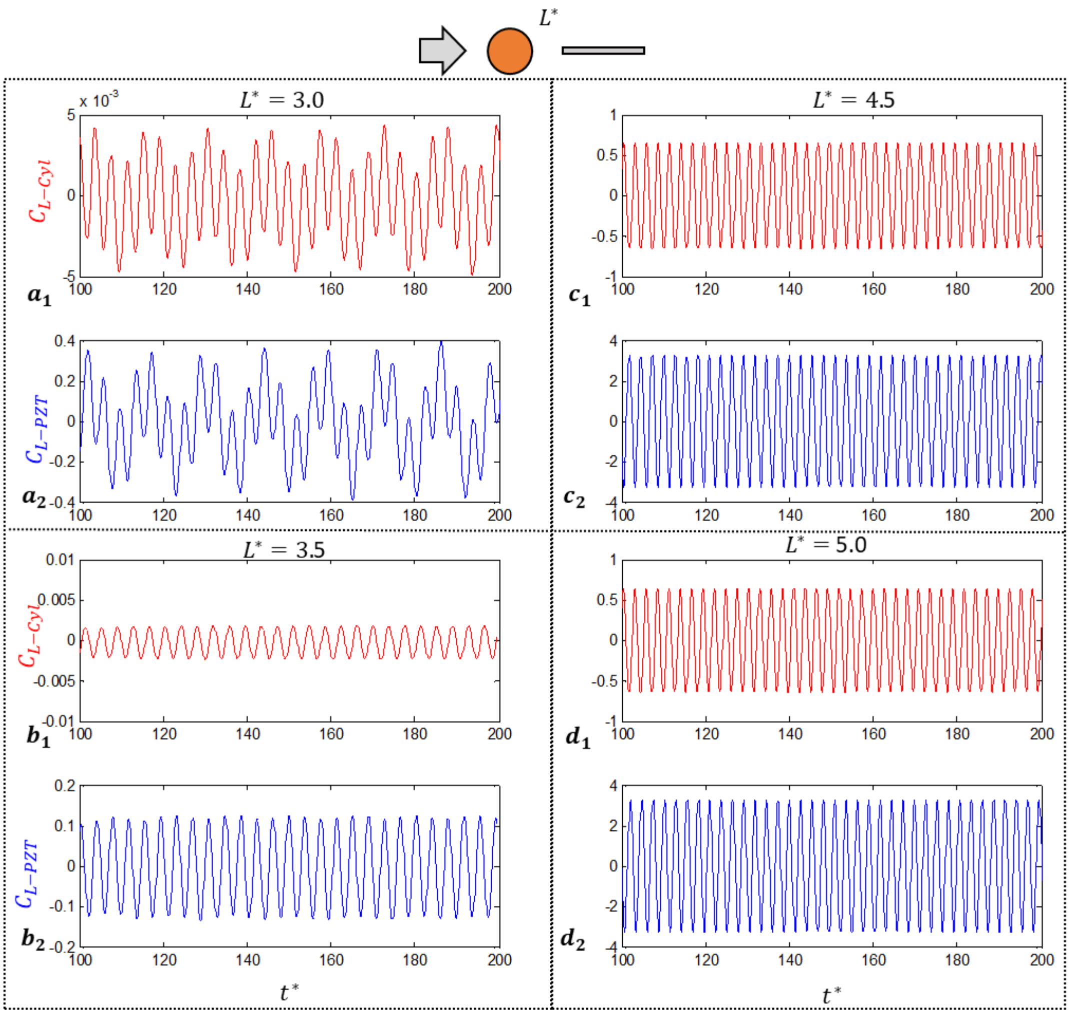

Figure 4 Time series of the lift coefficients of the cylinder and PZT as a function of gap ratio (L*) at Re = 200.

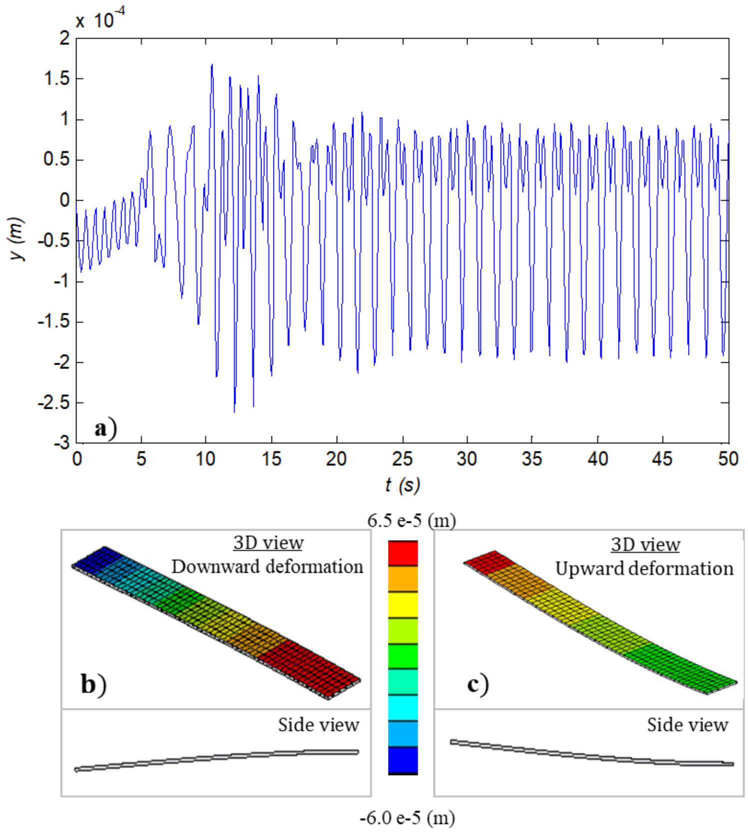

Figure 5 Deformation of the PZT actuator as a function of time when GR = L* = 4.0 and Re = 200.

CONCLUSIONS

A comprehensive investigation was conducted using numerical simulations to examine the laminar flow characteristics surrounding a combined configuration comprising a circular cylinder and a piezoelectric transducer for the purpose of harnessing vortex wake energy. A thin PZT can easily capture mechanical energy from upcoming vorices in the flow as a source of energy and convert it to the renewable energy. This energy conversion from ambient due to the vibration of PZT can be employed at a wide range of applications, such as microelectromechanical systems, underwater environments, where the WIV or VIV phenomena can be used for underwater energy harvesting, actuators, remote sensing applications, and wireless health monitoring sensors. The study involved the integration of fluidic and structural equations to analyze the dynamic response of the flexible plate known as PZT within the wake region of the upstream bluff body. Initially, the accuracy and reliability of the model were validated. The findings revealed that when the spacing ratio (L*) was less than or equal to 3.5, both the cylinder and the PZT experienced minimal lift forces. However, as the spacing ratio increased to 4.0, the applied lift forces on both the upstream cylinder and the PZT exhibited a significant increment. Subsequently, as the spacing ratio was further increased to values greater than or equal to 4.0, the fluctuating lift coefficient of the coupled cylinder-PZT system demonstrated negligible variation. It was deduced that the spacing ratio not only influenced the hydrodynamic coefficients but also can impact on the deformation and power output of the plate.

REFERENCES

Akaydın, H. D., Elvin, N., & Andreopoulos, Y. 2010. Wake of a cylinder: a paradigm for energy harvesting with piezoelectric materials. Experiments in Fluids, 49(1), 291-304.

Alam, M.M., Zheng, Q., Derakhshandeh, J.F., Rehman, S., Ji, C. and Zafar, F., 2018. On forces and phase lags between vortex sheddings from three tandem cylinders. International Journal of Heat and Fluid Flow, 69, pp.117-135.

Bernitsas, M.M., Raghavan, K., Ben-Simon, Y. and Garcia, E.M.H., 2008. VIVACE (Vortex Induced Vibration Aquatic Clean Energy): A new concept in generation of clean and renewable energy from fluid flow. Journal of offshore mechanics and Arctic engineering, 130(4).

Dai, H.L., Abdelkefi, A., Wang, L., 2014, Piezoelectric energy harvesting from concurrent vortex-induced vibrations and base excitations, Nonlinear Dynamics, 77, 967-981;

Dehkordi, B.G., Moghaddam, H.S. and Jafari, H.H., 2011. Numerical simulation of flow over two circular cylinders in tandem arrangement. Journal of Hydrodynamics, 23(1), pp.114-126.

Derakhshandeh, J.F., Arjomandi, M., Cazzolato, B.S. and Dally, B., 2014. Effect of a rigid wall on the vortex induced vibration of two staggered circular cylinders. Journal of Renewable and Sustainable Energy, 6(3), p.033114.

Derakhshandeh, J.F., Arjomandi, M., Dally, B. and Cazzolato, B., 2016. Flow-induced vibration of an elastically mounted airfoil under the influence of the wake of a circular cylinder. Experimental Thermal and Fluid Science, 74, pp.58-72.

Derakhshandeh, J.F. and Gharib, N., 2021. Numerical studies of laminar flow over two tandem elliptical cylinders using Ramanujan approximation. Journal of the Brazilian Society of Mechanical Sciences and Engineering, 43(3), p.169.

Hu, Y., Yang, B., Chen, X., Wang, X. and Liu, J., 2018. Modeling and experimental study of a piezoelectric energy harvester from vortex shedding-induced vibration. Energy conversion and management, 162, pp.145-158.

Koyvanich, K., Smithmaitrie, P. and Muensit, N., 2015. Perspective microscale piezoelectric harvester for converting flow energy in water way. Advanced Materials Letters, 6(6), pp.538-543.

Mehmood, A., Abdelkefi, A., Hajj, M.R., Nayfeh, A.H., Akhtar, I. and Nuhait, A.O., 2013. Piezoelectric energy harvesting from vortex-induced vibrations of circular cylinder. Journal of Sound and Vibration, 332(19), pp.4656-4667.

Meneghini, J.R., Saltara, F., Siqueira, C.L.R. and Ferrari Jr, J.A., 2001. Numerical simulation of flow interference between two circular cylinders in tandem and side-by-side arrangements. Journal of fluids and structures, 15(2), pp.327-350.

Meng, J., Fu, X., Yang, C., Zhang, L., Yang, X. and Song, R., 2021. Design and simulation investigation of piezoelectric energy harvester under wake-induced vibration coupling vortex-induced vibration. Ferroelectrics, 585(1), pp.128-138.

Ramm, E., & Wall, W. (1998). Fluid-structure interaction based upon a stabilized (ALE) finite element method. In 4th World Congress on Computational Mechanics: New Trends and Applications, CIMNE, Barcelona (pp. 1-20).

Sahu, T.R., Furquan, M., Jaiswal, Y. and Mittal, S., 2019. Flow-induced vibration of a circular cylinder with rigid splitter plate. Journal of Fluids and Structures, 89, pp.244-256.

Shan, X., Li, H., Yang, Y., Feng, J., Wang, Y. and Xie, T., 2019. Enhancing the performance of an underwater piezoelectric energy harvester based on flow-induced vibration. Energy, 172, pp.134-140.

Zhang, M. and Wang, J., 2016. Experimental study on piezoelectric energy harvesting from vortex-induced vibrations and wake-induced vibrations. Journal of Sensors, 2016.

Zhang, M., Zhang, C., Abdelkefi, A., Yu, H., Gaidai, O., Qin, X., Zhu, H. and Wang, J., 2021. Piezoelectric energy harvesting from vortex-induced vibration of a circular cylinder: Effect of Reynolds number. Ocean Engineering, 235, p.109378.

Zhao, D., Zhou, J., Tan, T., Yan, Z., Sun, W., Yin, J. and Zhang, W., 2021. Hydrokinetic piezoelectric energy harvesting by wake induced vibration. Energy, 220, p.119722.